THE JOURNAL OF PHYSICAL CHEMISTRY B

Article

pubs.acs.org/JPCB

Metal Cation Dependence of Interactions with Amino Acids: Bond Energies of Rb^+ and Cs^+ to Met, Phe, Tyr, and Trp

P. B. Armentrout,*[,†] Bo Yang,[‡] and M. T. Rodgers*[,‡]

[†]Department of Chemistry, University of Utah, 315 S. 1400 E. Rm 2020, Salt Lake City, Utah 84112, United States

[‡]Department of Chemistry, Wayne State University, Detroit, Michigan 48202, United States

Supporting Information

ABSTRACT: The interactions of rubidium and cesium cations with four amino acids (AA) including methionine (Met), phenylalanine (Phe), tyrosine (Tyr), and tryptophan (Trp) are examined in detail. Experimentally, the bond dissociation energies (BDEs) are determined using threshold collision-induced dissociation of the Rb^+(AA) and Cs^+(AA) complexes with xenon in a guided ion beam tandem mass spectrometer. Analyses of the energy dependent cross sections include consideration of unimolecular decay rates, internal energy of the reactant ions, and multiple ion-neutral collisions. 0 K BDEs of 121.0 ± 7.0 (102.8 ± 6.6), 123.8 ± 7.2 (112.9 ± 5.5), 125.8 ± 7.4 (115.6 ± 6.9), and 138.1 ± 7.5 (125.0 ± 6.8) kJ/mol are determined for complexes of Rb^+ (Cs^+) with Met, Phe, Tyr, and Trp, respectively. Quantum chemical calculations are conducted at the B3LYP, MP2(full), and M06 levels of theory with geometries and zero point energies calculated at the B3LYP level using def2-TZVPPD basis sets. Results obtained using all three levels show good agreement with experiment, with B3LYP values being systematically low and MP2(full) and M06 values being systematically high. At 0 and 298 K, theory predicts the ground-state conformers for M^+(Met) either have tridentate binding of the metal cation to the carbonyl, amino, and sulfur groups (MP2 and M06) or to both oxygens of a zwitterionic conformation (B3LYP). At 298 K, binding to the carboxylic acid group and the sulfur also becomes competitive. For the aromatic amino acids at 0 K, most levels of theory favor tridentate binding of the metal ions to the backbone carbonyl and amino groups along with the π-cloud of the ring, whereas for Rb^+(Trp) and Cs^+(AA), B3LYP theory favors binding to only the carbonyl and ring groups. At 298 K, B3LYP favors the latter binding mode for all three Rb^+(aromatic AA) complexes. Comparison of these results to those for the smaller alkali cations provides insight into the trends in binding affinities and structures associated with metal cation variations.

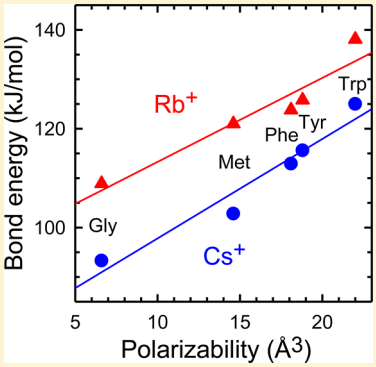

INTRODUCTION

As alkali metal cations, Rb^+ and Cs^+ follow the same biological pathways and bind at the same sites as K^+,[1,2] which along with Na^+, is an essential nutrient whose enzymatic transfer across cellular membranes is required for homeostasis and cellular function. The heavier Rb^+ and Cs^+ cations have different transport and accumulation rates,[3−6] sufficiently so that rubidium and cesium isotopes can be used in imaging of tissue and tumors without severe toxicity.[7] Cesium is also of interest because atmospheric testing of thermonuclear devices and nuclear reactor accidents have introduced radioactive cesium isotopes into the environment. Hence, as reviewed by Gal et al.,[8] an understanding of the interactions of these alkali metal cations with organic matter is useful. Despite this potential utility, the number of systems for which rubidium and cesium cation affinities are known is much smaller than for sodium and potassium.[8]

Clearly, the interactions of such cations with all relevant biological systems cannot be explicitly studied; however, insight into all such interactions can be approached by creating a "thermodynamic vocabulary" of specific pairwise interactions in small-scale systems.[9] Such quantitative information on a limited set of systems can then be combined to understand systems of greater complexity. Complications resulting from solvent effects can be eliminated by working in the gas phase, where the quantitative measurement of the intrinsic bond strengths between alkali metal cations and peptides can be directly measured. Gas phase information also allows detailed comparisons of experimental and theoretical results, which can help elucidate subtle features in how metal cation affinities vary with the identity of the metal cation. Such previous work[9,10] has found a correlation between the binding energies for Na^+ and K^+ to several amino acids and the polarizabilities of those amino acids. Included among the amino acids showing this correlation were glycine (Gly), methionine (Met), and the aromatic amino acids phenylalanine (Phe), tyrosine (Tyr), and tryptophan (Trp). Further, this correlation provides a baseline to better understand the effects of more polar side chains.[11,12] The present study was initiated in order to explore whether this correlation with polarizability continues for the heavier alkali metal cations.

Received: February 6, 2013
Revised: March 20, 2013
Published: March 20, 2013

Previously, we have studied the pairwise interactions of all five alkali-metal cations with Gly,[13−17] proline (Pro),[16−18] serine (Ser),[16,17,19] threonine (Thr),[16,17,19] and cysteine (Cys)[17,20] by examining their threshold collision-induced dissociation (TCID) using guided ion beam tandem mass spectrometry. Recent work has extended these studies to histidine (His) except for the Li^+ complex.[12] For Met, similar studies have been conducted for complexes with the lighter alkali metal cations, Li^+, Na^+, and K^+,[11] and for Phe, Tyr, and Trp, only complexes with Na^+ and K^+ have been examined in this fashion.[10] Quantitative bond dissociation energies (BDEs) were determined and found to be consistent with theoretical values predicted for the ground state conformations. Notably, studies of many of these complexes using infrared multiple photon dissociation (IRMPD) action spectroscopy find that the ground state geometries of metal cation amino acid complexes are sensitive to the metal cation identity. Although the entire sequence of alkali metal cations with Gly and Pro have not been examined by IRMPD,[21] such studies have found that the M^+ = Li^+ and Na^+ complexes are bound in tridentate conformers, [N,CO,OH] for M^+(Ser)[22] and M^+(Thr),[23] [N,CO,S] for M^+(Cys)[24] and M^+(Met),[25] [N,CO,CO] for M^+(Asn),[26] and [N,CO,N_π] for M^+(His)[27] (where the terms in brackets indicate the metal binding sites and N_π refers to the nearest side-chain nitrogen; see below for a more complete definition of the nomenclature used). Spectra for M^+ = K^+, Rb^+, and Cs^+ are more complicated and exhibit features associated with these tridentate conformers as well as unequivocal evidence of bidentate [COOH] conformations, and in the case of Met, a tridentate [COOH,S] conformer. For His, a bidentate [CO,N_π] conformer is dominant for the heavier metal cations. Additionally, the spectrum for cesiated serine clearly includes contributions from a zwitterionic [CO_2^-] conformer, which also may contribute to the spectra for threonine and cysteine complexes with Cs^+. For Met, such zwitterionic structures are clearly present for all three of the heavier alkali metal cations. For the strongly basic guanidine side-chain of arginine (Arg), M^+(Arg) are found to be zwitterionic for all alkali metal cations except Li^+, where again a tridentate conformer dominates.[28] For the aromatic amino acids of interest in the present work, IRMPD studies have demonstrated a similar trend. For M^+(Trp), Li^+ is exclusively tridentate [N,CO,R_π] where R_π indicates binding to the π-cloud of the ring, whereas the larger alkali cations exhibit an additional bidentate [CO,R_π] conformer, with comparable contributions for Rb^+ and Cs^+.[29] For M^+(Phe), the smaller cations, Li^+, Na^+, and K^+, are found to have exclusively [N,CO,R_π] conformers, with additions of [CO,R_π] for Rb^+ and Cs^+, and also [COOH] for Cs^+.[30] Of the tyrosine complexes, only K^+(Tyr) has been studied by IRMPD spectroscopy to date, but its results parallel those for K^+(Phe) closely (exclusive tridentate [N,CO,R_π] binding), and this trend is expected for the other alkali metal cations as well.[31]

In the work presented here, we extend our previous TCID studies to provide the first experimental values for Rb^+ and Cs^+ binding with methionine and the aromatic amino acids. Absolute BDEs of the Rb^+ (AA) and Cs^+ (AA) complexes, where AA = Met, Phe, Tyr, and Trp, are measured using TCID in a guided ion beam tandem mass spectrometer. Quantum chemical calculations at several levels of theory are carried out to provide structures, vibrational frequencies, and rotational constants needed for analysis of the TCID data. Several levels of theory are explored in order to provide theoretical BDEs in good agreement with experiment. Combined, the experimental and theoretical studies achieve a quantitative understanding of various effects (e.g., chelation, electron delocalization, inductive effects, and conformational strain) on the binding strength of all four ligands with the rubidium and cesium cations and how these effects differ from those associated with the lighter alkali metal cations.

EXPERIMENTAL AND COMPUTATIONAL SECTION

General Experimental Procedures. Cross sections for CID of the rubidium and cesium cation-amino acid complexes are measured using the Wayne State University guided ion beam tandem mass spectrometer that has been described in detail previously.[32] Experiments are conducted using an electrospray ionization (ESI) source[33] under conditions similar to those described previously.[17,33] Briefly, the ESI is operated using a 50:50 by volume H_2O/MeOH solution with $\sim 2 \times 10^{-4}$ M amino acid and $2-6 \times 10^{-4}$ M RbCl or CsCl (all chemicals purchased from Sigma-Aldrich). All other operating conditions are similar to those used previously. Notably the ESI/ion funnel/radio frequency (rf) hexapole source arrangement used here has been shown to produce ions thermalized to 300 K.[33−38] Additional details of the source can be found in the Supporting Information.

Rb^+(AA) or Cs^+(AA) complexes are extracted from the source, focused, accelerated, and mass selected using a magnetic momentum analyzer. The mass-selected ions are decelerated to a well-defined kinetic energy and focused into a rf octopole ion guide that traps the ions radially. The octopole passes through a static gas cell containing xenon, which is used as the collision gas because it is heavy and polarizable, leading to more efficient kinetic to internal energy transfer.[39,40] After collision, the reactant and product ions drift to the end of the octopole where they are extracted and focused into a quadrupole mass filter for mass analysis. The ions are detected with a high voltage dynode, scintillation ion detector[41] and the signal is processed using standard pulse counting techniques. Ion intensities, measured as a function of collision energy, are converted to absolute cross sections as described previously.[42] The uncertainty in relative cross sections is approximately ±5% and that for the absolute cross sections is approximately ±20%. The ion kinetic energy distribution is measured to be Gaussian and has a typical fwhm of 0.2−0.5 eV (lab). Uncertainties in the absolute energy scale are approximately ±0.05 eV (lab). Ion kinetic energies in the laboratory frame are converted to energies in the center-of-mass (CM) frame using $E_{CM} = E_{lab}[m/(m + M)]$, where M and m are the masses of the ionic and neutral reactants, respectively. All energies herein are reported in the CM frame unless otherwise noted.

Thermochemical Analysis. Threshold regions of the CID reaction cross sections are modeled using procedures developed elsewhere,[43−46] as described previously for similar systems.[13−16,18−20] Details of the analysis procedure, which includes explicitly accounting for internal and translation energy distributions, the effects of multiple collisions, and the lifetime of the dissociating ions, can be found in the Supporting Information.

Computational Details. All theoretical calculations were performed using Gaussian09.[47] Ground-state conformers of the four amino acids calculated at the levels of theory discussed below have been described previously.[10,11,48] Likely low-energy conformers of methionine,[25] phenylalanine,[30] and tryptophan[29] complexed with Rb^+ and Cs^+ have been examined in previous work whereas for tyrosine, structures previously found for

dx.doi.org/10.1021/jp401366g | J. Phys. Chem. B 2013, 117, 3771−3781

K^+(Tyr) are used as starting points for the present work.[10,49] In all cases, the structures have been reoptimized at the B3LYP/def2-TZVPPD level of theory,[50,51] which has been found to give good results for complexes of these alkali metal cations.[16,17,52] The def2-TZVPPD basis set[53,54] is a balanced basis set on all atoms at the triple-ζ level including polarization and diffuse functions and uses ECPs on rubidium and cesium developed by Leininger et al.[55] The def2-TZVPPD basis set was obtained from the EMSL basis set exchange library.[56,57] Geometry optimizations and vibrational frequencies were calculated at the B3LYP/def2-TZVPPD level with zero-point energies being scaled by 0.989.[58] Single point energies at this level as well as M06/def2-TZVPPD[59] and MP2(full)/def2-TZVPPD[60] levels using the B3LYP geometries were also calculated. Basis set superposition errors (BSSE) corrections at the full counterpoise (cp) level[61,62] were applied in all cases and ranged from <1.1 kJ/mol for the DFT calculations to 13−28 kJ/mol for Rb^+ complexes and 7−18 kJ/mol for Cs^+ complexes for the MP2(full) results. (Some insight into the large cp corrections needed for the MP2 full approach are provided in the Supporting Information.) It has been previously mentioned that the full counterpoise approximation to BSSE can provide worse agreement with experiment than MP2 theoretical values without BSSE corrections,[63−66] but previous experience with complexes of Cs^+ finds that cp corrections are needed.[17] Here, we also find that even with cp corrections, the MP2 values exceed experimental values, such that without cp corrections, the discrepancies are much worse (by an average of 20 kJ/mol). Therefore, all of the absolute binding energies reported here include cp corrections.

In previous studies of amino acids complexed with Rb^+ and Cs^+,[12,16,17,20] we also used the HW*/6-311+G(d,p) basis set where HW* indicates that Rb and Cs were described using the effective core potential (ECPs) and valence basis sets of Hay and Wadt[67] (equivalent to the LANL2DZ basis set) with a single d polarization function added.[68] In all cases,[12,16,17,20] this basis set is not large enough to adequately describe the energetics of the Rb^+ and Cs^+ complexes; hence, this basis set was not utilized here.

For several of the lowest energy conformers of each system, we also performed M06/def2-TZVPPD and M06-2X/def2-TZVPPD geometry optimizations and frequency calculations. Energies were again corrected for zero-point energies with frequencies scaled by 0.989 and full counterpoise corrections, which are $\leq$1.0 kJ/mol.

Conversion from 0 to 298 K and Excited Conformers. Conversion from 0 to 298 K thermochemistry is accomplished using the rigid rotor/harmonic oscillator approximation with rotational constants and vibrational frequencies calculated at the B3LYP/def2-TZVPPD level. Relative ΔG_{298} values for all conformers of these complexes are reported below. In general, the relative ΔG_{298} excitation energies are comparable to the analogous differences in the ΔH_0 values, although tridentate structures invariably have lower entropies than bidentate structures and therefore increase in relative free energy by up to 5 kJ/mol. Bond energies for the lowest energy species are also converted from our 0 K experimental thresholds to ΔH_{298} and ΔG_{298} values. Here uncertainties are determined by scaling most of the vibrational frequencies by ±10% along with 2-fold variations in the metal−ligand frequencies.

RESULTS

Theoretical Results. Structures of complexes of the four neutral amino acids with Rb^+ and Cs^+ experimentally studied here were calculated as described above. Figure 1 shows two low energy conformations for each system. Tables 1 and Supporting Information Table S1 provide more complete geometric and energetic information on these and other low-lying conformers. Energetic information is provided as both 0 and 298 K free energies, with the latter providing the basis for which structures might be populated experimentally. Previous work has discussed the structures of the M^+(Met), M^+(Phe), and M^+(Trp) complexes for M^+ = Rb^+ and Cs^+,[25,29,30] so only an abbreviated discussion is provided here. The nomenclature adopted here identifies the binding sites of the metal ion in brackets: the backbone amino nitrogen (N), the backbone carbonyl (CO), both oxygens of the carboxylic acid (COOH),

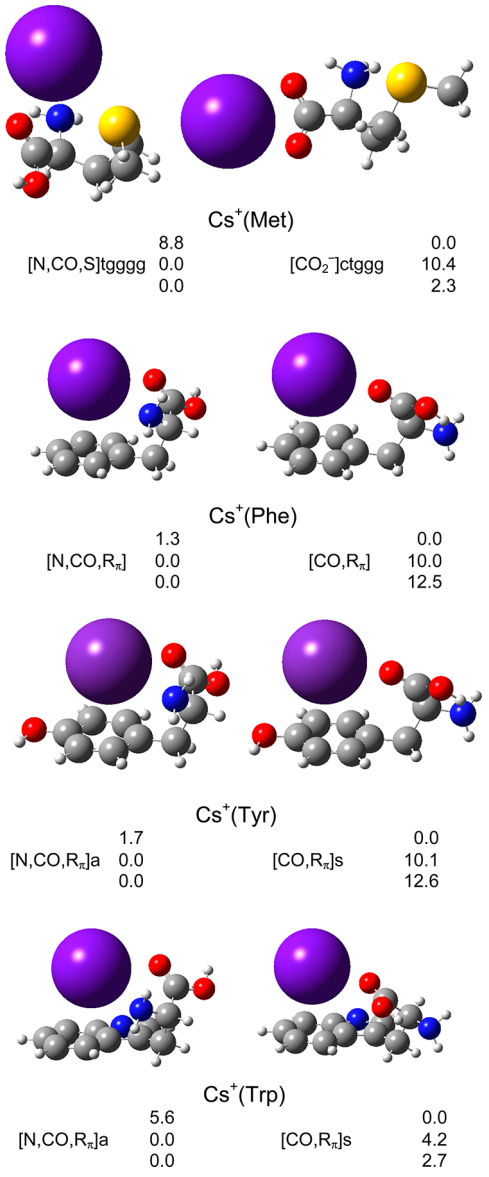

Figure 1. Low-energy structures of Cs^+(AA) calculated at the B3LYP/def2-TZVPPD level. Relative energies at 0 K in kJ/mol calculated at the B3LYP, M06, and MP2(full) (top to bottom) levels of theory using the def2-TZVPPD basis sets are shown.

dx.doi.org/10.1021/jp401366g | J. Phys. Chem. B 2013, 117, 3771−3781

Table 1. Bond Distances (Å), Bond Angles (deg), and Relative Free Energies at 0 (298) K for Low-Energy Structures of Rubidium and Cesium-Cation Bound Met, Phe, Tyr, and Trp[a]

structure	$r(M^+-O)^b$	$r(M^+-X)$	$r(M^+-Y)^c$	$\angle XM^+O^b$	$\angle XM^+Y^c$	$\angle O^bM^+Y^c$	relative energies (kJ/mol)[d] B3LYP	M06	MP2(full)	Lit.
M^+(Met)										
[N,CO,S]tgcgt	2.824	3.118[e]	3.440	55.6[e]	59.3[e]	81.3	1.9 (2.4)	**0.0** (**0.0**)	0.3 (**0.0**)	
	2.981	3.305	3.618	52.2	55.6	76.9	4.8 (5.1)	0.5 (**0.0**)	1.5 (0.1)	
[N,CO,S]tgggg	2.795	3.197[e]	3.471	53.7[e]	68.1[e]	72.3	7.6 (9.2)	1.0 (2.1)	**0.0** (0.8)	
	2.946	3.408	3.632	50.2	64.3	68.2	8.8 (10.6)	**0.0** (1.0)	**0.0** (0.1)	
[CO_2^-]cgtgg	2.791	2.888[f]		46.6[f]			0.2 (**0.0**)	13.4 (12.7)	8.3 (7.3)	
	2.926	3.041		44.2			0.3 (**0.0**)	13.6 (12.5)	6.1 (4.2)	
[CO_2^-]ctggg	2.803	2.874[f]		46.6[f]			**0.0** (0.3)	10.6 (10.4)	4.4 (3.9)	
	2.940	3.030		44.2			**0.0** (0.2)	10.4 (9.8)	2.3 (0.8)	
[COOH,S]cgggg	2.829	3.048[f]	3.638	44.2[f]	65.3[f]	66.9	6.4 (6.0)	3.5 (2.6)	3.5 (2.3)	
	2.966	3.250	3.843	41.5	61.5	63.0	5.8 (5.5)	2.8 (1.8)	1.9 (**0.0**)	
M^+(Phe)										
[N,CO,R_π]	2.839	3.139[e]	3.469(C_1)	54.8[e]	54.2[e]	67.2	**0.0** (2.9)	**0.0** (**0.0**)	**0.0** (**0.0**)	**0** (5)[30]
	2.992	3.315	3.673(C_1)	51.7	51.2	63.3	1.3 (6.4)	**0.0** (**0.0**)	**0.0** (**0.0**)	2 (10)
[CO,R_π]	2.686		3.495(C_4)			98.4	0.3 (**0.0**)	9.7 (6.5)	13.7 (10.5)	1 (1)
	2.836		3.695(C_4)			92.7	**0.0** (1.7)	10.0 (6.7)	12.5 (9.2)	**0** (4)
[COOH]cgt	2.805	3.142[f]		43.3[f]			4.8 (0.8)	21.4 (14.5)	36.6 (29.7)	6 (**0**)
	2.938	3.428		39.9			1.4 (**0.0**)	21.1 (14.6)	31.6 (25.1)	1 (**0**)
[COOH]cgg	2.847	3.030[f]	3.756(C_2)	44.2[f]	68.5[f]	58.8	13.3 (11.7)	19.2 (14.7)	25.8 (21.2)	6 (4)
	2.966	3.282	5.510(C_2)	41.2			3.6 (4.5)	20.6 (16.4)	27.4 (23.2)	2 (4)
M^+(Tyr)										
[N,CO,R_π]a	2.839	3.129[e]	3.437(C_2)	55.0[e]	61.5[e]	89.1	**0.0** (3.3)	**0.0** (**0.0**)	**0.0** (**0.0**)	
	2.991	3.309	3.615(C_2)	51.7	51.5	84.2	1.7 (6.4)	**0.0** (**0.0**)	**0.0** (**0.0**)	
[CO,R_π]s	2.691		3.437(C_3)			86.1	0.6 (**0.0**)	10.6 (6.8)	13.6 (9.8)	
	2.841		3.636(C_3)			87.3	**0.0** (**0.0**)	10.1 (5.5)	12.6 (8.0)	
[N,CO,R_π]s	2.834	3.132[e]	3.457(C_1)	55.0[e]	54.4[e]	67.5	0.5 (3.9)	0.7 (0.9)	0.0_3 (0.2)	
	2.984	3.312	3.658(C_1)	51.8	51.4	63.7	2.4 (7.0)	0.7 (0.7)	0.5 (0.5)	
[CO,R_π]a	2.687		3.480(C_4)			98.2	1.0 (0.9)	10.1 (6.7)	12.5 (9.1)	
	2.838		3.669(C_4)			91.4	0.9 (1.8)	10.0 (6.2)	11.5 (7.7)	
[COOH]cggs	2.849	3.043[f]	3.717(C_2)	44.1[f]	68.2[f]	59.0	11.0 (9.9)	16.9 (12.6)	22.4 (18.0)	
	2.957	3.296	5.447(C_2)	41.1	48.0	36.6	3.2 (1.4)	19.3 (12.8)	26.1 (19.6)	
[COOH]cgts	2.802	3.138[f]		43.4[f]			4.9 (1.6)	21.6 (15.1)	36.2 (29.8)	
	2.935	3.424		39.9			2.1 (0.3)	21.0 (14.5)	31.7 (25.3)	
M^+(Trp)										
[N,CO,R_π]a	2.858	3.132[e]	3.297(C_{3a})	54.5[e]	65.9[e]	83.0	4.0 (4.9)	**0.0** (**0.0**)	**0.0** (**0.0**)	4 (4)[29]
	3.023	3.320	3.453(C_{3a})	51.1	61.9	79.5	5.6 (7.9)	**0.0** (**0.0**)	**0.0** (**0.0**)	6 (6)
[CO,R_π]s	2.720		3.398(C_4)			69.4	**0.0** (**0.0**)	3.6 (2.6)	3.0 (2.0)	**0** (**0**)
	2.876		3.576(C_5)			88.6	**0.0** (**0.0**)	4.2 (1.9)	2.7 (0.4)	**0** (**0**)
[CO,R_π]a	2.718		3.423(C_{3a})			66.0	3.3 (4.0)	7.0 (6.7)	5.7 (5.4)	3 (3)
	2.869		3.619(C_{3a})			62.4	3.4 (4.8)	6.9 (6.1)	5.6 (4.7)	3 (3)
[N,CO,R_π]s	2.823	3.165[e]	3.328(C_{3a})	54.6[e]	69.4[e]	76.3	9.5 (10.1)	6.3 (5.9)	6.7 (6.3)	9 (9)
	2.979	3.357	3.488(C_{3a})	51.2	65.8	72.4	10.8 (12.5)	6.0 (5.4)	6.0 (5.4)	12 (12)
[COOH,R_π]s	2.855	3.089[f]	3.425(C_4)	43.6[f]	80.1[f]	61.0	4.6 (4.5)	7.3 (6.3)	9.9 (8.9)	
	2.998	3.292	3.638(C_4)	41.0	76.4	57.6	4.0 (4.9)	8.4 (7.1)	10.2 (8.9)	

[a]Upper and lower values correspond to Rb^+ and Cs^+, respectively. Geometries indicate ground state of theory. Values in bold optimized at M06/def2-TZVPPD level. [b]Carbonyl oxygen of the amino acid backbone. [c]Y = sulfur or ring carbon (noted) of the amino acid side chain. [d]Relative free energies at 0 (298) K determined at the indicated level of theory with the def2-TZVPPD basis set using the associated B3LYP geometry. [e]X = amino nitrogen. [f]X = hydroxyl oxygen of the amino acid backbone (or hydrogen bonded oxygen in zwitterionic conformers).

both oxygens of a zwitterionic carboxylate (CO_2^-), the sulfur of the Met side chain (S), or the aromatic rings of Phe, Tyr, and Trp (R). For M^+(Met), there are a diverse set of alternative conformers, which are designated by noting the approximate dihedral angles of ∠HOCC, ∠OCCC, ∠CCCC, ∠CCCS, and ∠CCSC (designated as c for cis, <50°; t for trans, >135°; and g for gauche, all angles in between) with + and − subscripts to indicate the sign on gauche angles when needed to differentiate conformers. For complexes of Phe, the binding sites are sufficient to differentiate most of the low-energy conformers, except that the [COOH] and [CO_2^-] have both cgg and cgt variants, which designate the ∠HOCC, ∠OCCC, and ∠CCCC dihedral angles. Such designations are also needed for the other two aromatic amino acids, where Trp requires adding the ∠CCCC(N) dihedral. In addition, Tyr and Trp have asymmetric side chains such that flipping the ring over allows

dx.doi.org/10.1021/jp401366g | J. Phys. Chem. B 2013, 117, 3771−3781

an alternative conformation. For Tyr, the distinction is the direction of the hydroxyl hydrogen on the phenol side chain, which we designate with respect to the amino group as syn (s) (on the same side of the plane bisecting the ring and phenolic hydroxyl group) or anti (a) (on the opposite side). For Trp, the distinction lies in which side the indole nitrogen lies, which we again designate as s or a relative to the amino group.

M06 geometries, reported in Supporting Information Table S1, are similar to the B3LYP results although M06 bond lengths are shorter than the B3LYP bonds with the only exception being Rb^+(Tyr) [CO,R_π]s. M^+−OC bond lengths are an average of 0.03 ± 0.02 Å shorter, whereas M^+−N range from 0.04−0.14 Å shorter, M^+−S bond lengths are 0.06−0.11 Å shorter, and those for M^+−R (side-chain) are 0.04−0.21 Å shorter. Relative energies calculated at the M06//M06 versus M06//B3LYP levels are the same within 3 kJ/mol in all cases (14 systems) with an average difference of 1.1 ± 1.0 kJ/mol. Results calculated using the M06-2X approach, designed for main group elements in particular but not transition metals,[59] yielded bond energies 10−14 kJ/mol higher in energy than the M06 results for the aromatic amino acids and about 6 kJ/mol higher for Met. As will be seen below, this would make the M06-2X results in the poorest agreement with experiment. Bond energies calculated at the M06//M06 and M06-2x//M06-2x levels are compared with the B3LYP//B3LYP, M06//B3LYP, and MP2(full)//B3LYP values in Table S2 of the Supporting Information.

For the aromatic amino acids, all levels of theory agree on the conformation of the neutral ligand, which has been previously described.[10] For methionine, there are a variety of low-lying conformers, which again have been previously described.[11] Key differences relate to the hydrogen bonding where N1 conformers have NH···OC and OH···OC hydrogen bonds, whereas N2 conformers have a OH···N hydrogen bond. Variations in the orientation of the $-C_2H_4SCH_3$ side-chain are indicated by the ∠CCCS and ∠CCSC dihedral angles (designated as g = gauche or t = trans). At the B3LYP, M06, and MP2(full) levels using the def2-TZVPPD basis set, the ground states are N1-tg, N1-gt, and N2-g_g. In the data analysis, results are interpreted self-consistently such that the ground-state metal cation-amino acid complex is assumed to dissociate to the ground-state methionine conformer, where both are calculated at the same level of theory. Differences in the results for the two N1 conformers are negligible.

The methionine complexes exhibit the largest range of structural diversity. B3LYP finds four different binding motifs (each having at least two conformational variations) within ∼10 kJ/mol of the ground state: [CO_2^-], [N,CO,S], [COOH,S], and [COOH]. The 298 K ground state for both metal cations is [CO_2^-]cgtgg, with the [CO_2^-]ctggg conformer being nearly isoenergetic and the 0 K ground state. These calculations would indicate appreciable populations (>10%) of these conformers along with [N,CO,S]tgcgt and [COOH,S]cgggt for Rb^+(Met) and both [COOH] conformers as well for Cs^+(Met). M06 and MP2(full) calculations raise the relative energies of the [CO_2^-] and [COOH] conformers such that [N,CO,S]tgcgt is the 298 K ground state. Both [N,CO,S] and both [COOH,S] conformers are appreciably populated given the energetics at these levels of theory for both Rb^+(Met) and Cs^+(Met) with [CO_2^-]cgtgg also populated for Cs^+(Met) according to MP2 theory. As noted above, IRMPD studies are interpreted to indicate that both Rb^+(Met) and Cs^+(Met) conclusively show evidence of [N,CO,S] and [CO_2^-] conformers with contributions from [COOH,S] and [COOH] being possible. This is inconsistent with the M06 relative energetics and more consistent with B3LYP and MP2(full) results.

At the M06 and MP2(full) levels of theory, M^+(Phe) is predicted to have the [N,CO,R_π] tridentate structure with all other conformers lying >6 kJ/mol higher in energy, such that their 298 K populations would be small (<7%). In contrast, B3LYP results indicate that Rb^+(Phe) has a [CO,R_π] 298 K ground state, with [COOH] lying less than 1 kJ/mol higher in energy and [N,CO,R_π] lying about 3 kJ/mol higher, such that all three would be populated at 298 K. For Cs^+(Phe), the 298 K ground state switches to [COOH] with a low-lying [CO,R_π] conformer. The B3LYP results in Table 1 are similar to the computations of Dunbar et al. at the B3LYP/6-311+G(d,p) level using the SDD relativistic ECP on Rb and Cs.[30] In this work, IRMPD spectra of Rb^+(Phe) and Cs^+(Phe) were similar and complex, clearly indicating the presence of the [N,CO,R_π] complexes along with either [CO,R_π] or one of the [COOH] conformers, but no evidence for [CO_2^-]. This is not consistent with predictions of the M06 or MP2(full) levels, but the B3LYP predicted population for [N,CO,R_π] is also smaller than suggested by the spectra. Dunbar et al. showed this more definitively for the K^+(Phe) spectrum that was only consistent with the tridentate conformer, but their B3LYP calculations suggested a bidentate [CO,R_π] conformer should be competitive.

A similar situation occurs for the Tyr complexes, where M06 and MP2(full) predict [N,CO,R_π] ground states (0 and 298 K) with all other conformers lying >5 kJ/mol higher in energy at 298 K (and 10 kJ/mol at 0 K). The syn and anti [N,CO,R_π] variants lie within 1 kJ/mol of one another, consistent with Dunbar's conclusion that this variation is negligible.[49] In contrast, B3LYP indicates that [CO,R_π]s is the ground state (with the anti conformer being within 2 kJ/mol) along with low-energy [COOH]cgts and [COOH]cgta conformers. Thus, the different levels of theory predict very different distributions of conformers present at 298 K.

For tryptophan, M06 and MP2(full) again find tridentate [N,CO,R_π]a conformers as the 0 and 298 K ground state, with its syn conformer lying 5−7 kJ/mol higher in energy at 0 and 298 K. The bidentate [CO,R_π]s conformers lie 0.4−3 kJ/mol higher (3−4 kJ/mol at 0 K) with the [CO,R_π]a conformers at 5−7 kJ/mol above the ground state. [COOH,R_π]s is also relatively low lying at 6−9 kJ/mol above the ground state. All other conformers lie at least 20 kJ/mol above the ground state. At the B3LYP level, the same five conformers are low in energy but their order changes. Now, [CO,R_π]s is the ground state at both 0 and 298 K with [N,CO,R_π]a and [CO,R_π]a being 4−8 kJ/mol higher, [COOH,R_π]s lying 4−5 kJ/mol higher, and [N,CO,R_π]s lying 10−13 kJ/mol above the ground state. The latter results agree with the B3LYP calculations of Polfer et al.,[29] where IRMPD spectra demonstrated the presence of both [N,CO,R_π] and [CO,R_π] structures for both Rb^+(Trp) and Cs^+(Trp). This experimental result is consistent with all three levels of theory considered here.

Cross Sections for Collision-Induced Dissociation. Kinetic energy-dependent experimental cross sections were obtained for the interaction of Xe with M^+(AA) where M^+ = Rb^+ and Cs^+ and AA = Met, Phe, Tyr, and Trp. Figure 2 shows a representative data set for Rb^+(Met) and Supporting Information Figure S1 shows results for all eight M^+(AA) systems. For all eight complexes, the only dissociation pathway

dx.doi.org/10.1021/jp401366g | J. Phys. Chem. B 2013, 117, 3771−3781

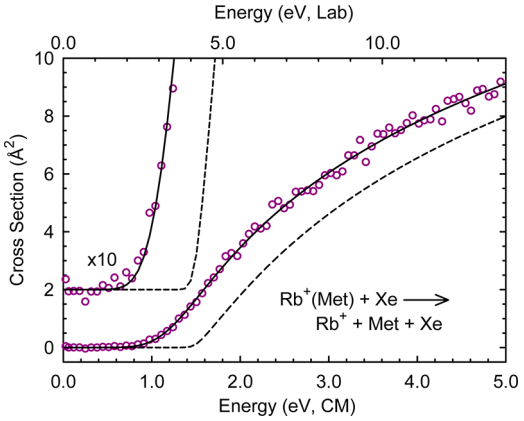

Figure 2. Cross sections for collision-induced dissociation of Rb^+(Met) with xenon as a function of kinetic energy in the center-of-mass frame (lower *x*-axis) and the laboratory frame (upper *x*-axis). Solid lines show the best fit to the data using the model of Supporting Information eq S2 convoluted over the neutral and ion kinetic and internal energy distributions. Dashed lines show the model cross sections in the absence of experimental kinetic energy broadening for reactant ions with an internal energy of 0 K. The data and models are shown expanded by a factor of 10 and offset from zero in the inset.

observed was the loss of the intact ligand in the collision-induced dissociation (CID) reactions 1

$$M^+(AA) + Xe \rightarrow M^+ + AA + Xe \quad (1)$$

Data shown are zero-pressure extrapolated results. Although the pressure dependence of these cross sections is small in all cases, thresholds measured at our highest pressure of 0.2 mTorr can exhibit lower thresholds than the zero-pressure cross sections by as much as 0.14 eV.

The models of Supporting Information eqs S1 (no lifetime effects) and S2 (lifetime effects included) were used to analyze zero pressure extrapolated cross sections for reactions 1 for the eight M^+(AA) systems. Typical models are shown in Figure 2 and Supporting Information Figure S1, which show that all experimental cross sections are reproduced by Supporting Information eq S2 over a large range of energies (>3 eV) and magnitudes (>2 orders of magnitude). The optimized fitting parameters of Supporting Information eqs S1 and S2 are provided in Table 2. In all systems, analyses were performed using molecular parameters for all structures that theory indicates could be the ground state (see previous section). Kinetic shifts are observed in all systems and range from ~0.1 eV for Cs^+(Met), the most weakly bound system, to about 0.6 eV for Rb^+(Trp), the most strongly bound system. The values of $\Delta S^{\dagger}_{1000}$, the entropy of activation at 1000 K, are also derived, which gives some idea of the looseness of the transition states. These values, listed in Table 2, are in the range determined by Lifshitz[69] for simple bond cleavage dissociations. This is reasonable considering that the TS is assumed to lie at the centrifugal barrier for the association of M^+ + AA.

As already included in the present analysis, we investigated the effect of having a different conformer populating the M^+(AA) cations generated in the electrospray ion source. In the case of methionine, different conformers of the Met product were also considered, as described above. The only fitting parameter to change significantly is the threshold energy, E_0.

Table 2. Fitting Parameters of Supporting Information Equations S1 and S2 and Entropies of Activation at 1000 K for CID of Rb^+(AA) and Cs^+(AA) for AA = Met, Phe, Tyr, and Trp[a]

				E_0 (no RRKM)	E_0 (PSL)	$\Delta S^{\dagger}_{1000}$
reactant	complex/ligand structure	σ_0	n	(eV)	(eV)	(J/K mol)
Rb^+(Met)	[N,CO,S]/N2	9.5 (1.8)	1.2 (0.1)	1.46 (0.07)	1.24 (0.07)	40 (2)
	[N,CO,S]/N1				1.27 (0.07)	58 (2)
	[CO_2^-]/N1				1.27 (0.07)	58 (2)
	[COOH,S]/N2				1.21 (0.07)	25 (2)
Rb^+(Phe)	[N,CO,R_π]	2.7 (0.4)	1.4 (0.1)	1.62 (0.07)	1.30 (0.07)	45 (2)
	[CO,R_π]				1.26 (0.07)	33 (2)
Rb^+(Tyr)	[N,CO,R_π]a	5.5 (0.9)	1.2 (0.1)	1.76 (0.07)	1.33 (0.07)	43 (2)
	[CO,R_π]s				1.28 (0.07)	28 (2)
	[COOH]cgts				1.25 (0.07)	12 (2)
Rb^+(Trp)	[N,CO,R_π]a	3.6 (0.5)	1.1 (0.1)	1.99 (0.07)	1.41 (0.07)	44 (2)
	[CO,R_π]s				1.45 (0.07)	42 (2)
	[COOH,R_π]s				1.44 (0.07)	46 (2)
Cs^+(Met)	[N,CO,S]/N2	5.1 (0.7)	1.3 (0.1)	1.15 (0.07)	1.06 (0.07)	33 (2)
	[N,CO,S]/N1				1.08 (0.07)	52 (2)
	[CO_2^-]/N1				1.08 (0.07)	52 (2)
	[COOH,S]/N2				1.04 (0.07)	25 (2)
Cs^+(Phe)	[N,CO,R_π]	3.7 (1.8)	1.3 (0.1)	1.42 (0.05)	1.19 (0.05)	44 (2)
	[CO,R_π]				1.17 (0.05)	29 (2)
	[COOH]cgt				1.15 (0.05)	11 (2)
Cs^+(Tyr)	[N,CO,R_π]a	3.8 (0.8)	1.0 (0.1)	1.58 (0.06)	1.22 (0.06)	44 (2)
	[CO,R_π]s				1.18 (0.06)	24 (2)
	[COOH]cgts				1.16 (0.06)	11 (2)
Cs^+(Trp)	[N,CO,R_π]a	2.6 (0.4)	1.0 (0.2)	1.79 (0.07)	1.29 (0.07)	46 (2)
	[CO,R_π]s				1.31 (0.07)	36 (2)
	[COOH,R_π]s				1.29 (0.07)	40 (2)

[a]Uncertainties (1 standard deviation) in parentheses.

dx.doi.org/10.1021/jp401366g | J. Phys. Chem. B 2013, 117, 3771−3781

Differences in the threshold energies among different conformers range from 0.02 to 0.08 eV, Table 2, and are generally within the overall experimental uncertainty of any individual measurement. These shifts occur because of differences in the kinetics of dissociation, as can also be seen by examining the entropies of activation. Lower entropies of activation are generally correlated with lower thresholds because there is a larger kinetic shift associated with the more restricted dissociation process. Overall, even though multiple conformations are probably formed in the source, as indicated by IRMPD results,[25,29,30] the bond energies obtained are largely insensitive to this because the energy content of the different conformers is approximately equal and differences in the unimolecular dissociation kinetics are small. In addition, a distribution of conformers is also effectively included in the analysis as the thermal distribution of internal energies available to the reactant ions. Because theory is not definitive with regard to the ground-state conformation, our best bond energies for all cases are the averages of values from all reasonable interpretations, Table 3, with differences associated with different conformers included in the final uncertainties. Furthermore, direct comparisons of experimental results for specific conformers with theoretical values at specific levels of theory in a self-consistent fashion do not provide a better comparison than the average values. Finally, the 0 K bond energies are converted to 298 K bond enthalpies and 298 K free energies of dissociation, conversions that also depend on the specific conformers involved. Table S3 of the Supporting Information contains a full exposition of these values.

Table 3. Experimental and Theoretical Rubidium and Cesium Cation Affinities of Met, Phe, Tyr, and Trp at 0 K (kJ/mol)

complex	experiment[a]	B3LYP[b]	M06[b]	MP2(full)[b]
Rb^+(Met)	121.0 (7.0)	116.9	127.8	123.7
Cs^+(Met)	102.8 (6.6)	104.3	118.1	114.4
Rb^+(Phe)	123.8 (7.2)	117.0	133.1	132.9
Cs^+(Phe)	112.9 (5.5)	104.1	125.1	125.4
Rb^+(Tyr)	125.8 (7.4)	117.8	134.3	133.1
Cs^+(Tyr)	115.6 (6.9)	105.3	126.0	125.6
Rb^+(Trp)	138.1 (7.5)	129.3	140.5	141.2
Cs^+(Trp)	125.0 (6.8)	116.3	133.4	135.1
MAD (Rb)[c]		6.9 (2.1)	6.8 (3.1)	5.5 (3.1)
MAD (Cs)[c]		7.3 (4.0)	11.6 (2.9)	11.0 (1.2)
MAD (all)[c]		7.1 (2.9)	9.2 (3.8)	8.3 (3.7)

[a]Present experimental values from Table 2 as averages of all conformations considered. Uncertainties (one standard deviation) in parentheses. [b]Calculations performed at the stated level of theory using the def2-TZVPPD basis set on all atoms with geometries and vibrational frequencies calculated at the B3LYP/def2-TZVPPD level. All values counterpoise corrected. [c]Mean absolute deviation from experimental values.

DISCUSSION

Comparison of Theoretical and Experimental Bond Dissociation Energies. The theoretical BDEs for the Rb^+(AA) and Cs^+(AA) complexes, where AA = Met, Phe, Tyr, and Trp, calculated at several levels of theory are compared to the experimental values in Table 3. Experiment indicates the relative BDEs increase in the order Met < Phe ≈ Tyr < Trp, which is in reasonable agreement with all levels of theory. The predicted range between the lowest (Met) and highest (Trp) experimental BDEs is 17 (22) kJ/mol for Rb^+ (Cs^+), compared to theoretical ranges at the B3LYP, M06, and MP2(full) levels of 12 (12), 13 (15), and 17 (21) kJ/mol, respectively. Clearly, MP2(full) predicts this trend the best, although B3LYP yields the lowest overall mean absolute deviation between theory and experiment at 7 ± 3 kJ/mol, with MP2(full) at 8 ± 4 and M06 at 9 ± 4 kJ/mol. All of these MADs are comparable to the average experimental uncertainty of 7 ± 1 kJ/mol.

It is perhaps worth noting that MP2(full) does a slightly better job of predicting the Rb^+(AA) BDEs with a MAD of 6 ± 3 kJ/mol compared to 7 ± 3 kJ/mol for B3LYP and M06; whereas B3LYP predicts the Cs^+(AA) BDEs the best with a MAD of 7 ± 4 kJ/mol compared to MP2(full) at 11 ± 1 and M06 at 12 ± 3 kJ/mol. These deviations are somewhat larger than those found previously for binding these alkali cations with other amino acids, Gly, Pro, Ser, Thr, Cys, and His.[12,16,17,20] For Rb^+ complexes, previous work on all but His was performed using the def2-TZVP basis set; hence, bond energies for these complexes along with those at the M06 level were recalculated here using the def2-TZVPPD basis set. The B3LYP/def2-TZVPPD bond energies are slightly smaller than the B3LYP/def2-TZVP literature values (by an average of 1.2 ± 0.7 kJ/mol), whereas the MP2(full)/def2-TZVPPD bond energies are slightly larger (by an average of 1.9 ± 0.9 kJ/mol (8.0 ± 2.2 kJ/mol without counterpoise corrections). For rubidium cation complexes of these six amino acids, the MADs compared to experiment are 4 ± 2 kJ/mol for B3LYP, 6 ± 3 kJ/mol for M06, and 3 ± 2 kJ/mol for MP2(full) approaches. For Cs^+ complexes (where all literature values already used the def2-TZVPPD basis set), MADs are 3 ± 3, 5 ± 3, and 5 ± 3 kJ/mol, respectively. For all ten amino acids, the MADs for Rb^+ complexes are 5 ± 3, 6 ± 3, and 4 ± 3 kJ/mol, respectively, and 5 ± 4, 8 ± 4, and 8 ± 4 kJ/mol, respectively, for Cs^+ complexes. For both metals and all ten amino acids, MADs are 5 ± 3, 7 ± 4, and 6 ± 4 kJ/mol, respectively.

Figure 3 illustrates the overall agreement between experiment and the B3LYP and MP2(full)/def2-TZVPPD results for the present systems. It can be seen that these results are

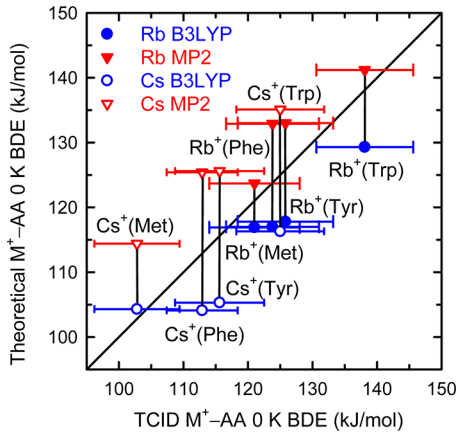

Figure 3. Experimental 0 K bond dissociation energies (in kJ/mol) for M^+(Met), M^+(Phe), M^+(Tyr), and M^+(Trp) for M^+ = Rb^+ (solid symbols) and Cs^+ (open symbols) plotted versus B3LYP/def2-TZVPPD (blue) and MP2(full)/def2-TZVPPD//B3LYP/def2-TZVPPD (red) theoretical values for the calculated ground state species. The diagonal line shows perfect agreement.

dx.doi.org/10.1021/jp401366g | J. Phys. Chem. B 2013, 117, 3771−3781

approximately within experimental error for all values, which is also true for the M06 level of theory as it provides results similar to MP2. Figure 3 also shows that the B3LYP values systematically underestimate the experimental values except for Cs^+(Met), whereas MP2(full) (and M06) overestimate them. It would appear that B3LYP provides good relative values for the three aromatic amino acids, but incorrectly increases the M^+(Met) BDE relative to these. The trends in the MP2(full) values better predict the observed experimental results.

Trends in Bond Energies: Metal Cation Identity and Side-Chain Substituents. Metal cations interact with amino acids by electrostatic ion induced-dipole, ion-quadrupole, and ion-dipole forces that lead to solvation of the charge by coordination of the functional groups of the amino acids. Our results for the BDEs required to remove the rubidium or cesium cation from M^+(AA), where AA = Met, Phe, Tyr, and Trp (Table 3), are smaller than the values for analogous complexes with $M^+ = Na^+$ and K^+,[10,11] as shown in Figure 4.

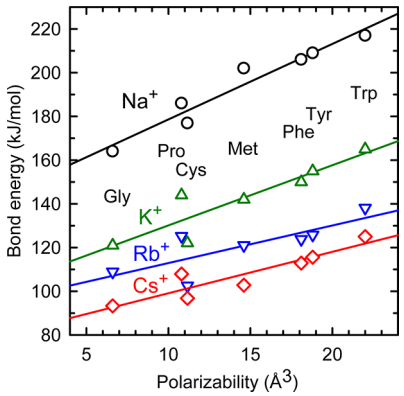

Figure 4. Experimental 0 K bond dissociation energies (in kJ/mol) for M^+(Gly), M^+(Pro), M^+(Cys), M^+(Met), M^+(Phe), M^+(Tyr), and M^+(Trp) for $M^+ = Na^+$ (circles), K^+ (triangles), Rb^+ (inverted triangles), and Cs^+ (diamonds) are plotted versus the calculated polarizability volume of the amino acid (in Å^3). The lines are linear regression fits to data for each metal cation.

Indeed, the bond energies decrease systematically from Na^+ to Cs^+ because the electrostatic interactions decrease with the increasing bond distances necessitated by the increasing size of the metal cation (radii of 0.98, 1.33, 1.49, and 1.69 Å, respectively[70]). Figure 4 also illustrates one of the primary rationales for the present study, that is, to establish the effect of ligand polarizability on the BDEs of the alkali metal cations to amino acids. As noted above, we have previously found a correlation between the binding energies of Gly, Pro, Met, Phe, Tyr, and Trp to Na^+ and K^+ and the polarizabilities of these amino acids.[9,10] This correlation has then allowed a more accurate assessment of the extra binding obtained from more polar side chains for these two metals,[12,19,35,71] but such a baseline has not been available for Rb^+ and Cs^+. Figure 4 reproduces these correlations including Cys. It can be seen that the BDEs for Rb^+(AA) and Cs^+(AA) to these seven amino acids follow similar trends established by Na^+(AA) and K^+(AA), consistent with the hypothesis regarding polarizability. Notably the slopes of the regression lines generally decline as the metal cation gets larger, consistent with a reduced effect resulting from the longer metal ligand bonds. It might also be important to notice that the Pro values are systematically higher than the correlation lines, whereas those for Cys are systematically lower, however, removing these points yields very similar correlations. The enhancement observed for Pro is probably a result of the zwitterionic structure of all four M^+(Pro) complexes,[16−18] such that the metal ion interacts with a polar ligand in contrast to the charge solvated structures of the other amino acids.

The ability to include the two amino acids containing sulfur side chains in this correlation attests to the relatively nonpolar character of the sulfur atom. This contrasts with the oxygen-based side chains of serine and threonine, where appreciable enhancements above the polarization effects can be found.[11,12] The fact that Met falls on the correlation line can probably be related to the longer side chain of Met versus Cys, such that the three coordinate [N,CO,X] structure is shared by Met, Phe, Tyr, and Trp, even for the larger metal cations. As discussed previously, the shorter side chain of Cys means that the larger metal cations cannot bind as effectively to the side chain while simultaneously binding to the preferred amino and carbonyl groups of the backbone.[20] Hence, alternative structures, like [COOH], become isoenergetic, which may explain why the M^+(Cys) values are decreased, especially for K^+ and Rb^+, compared to the aliphatic side chains, Figure 4.

Trends in Bond Energies: Effects of Polar Side Chains on Rb^+(AA) and Cs^+(AA). Having now established the correlation between polarizability of the amino acid and the binding energy to Rb^+ and Cs^+, the influence of polar side chains can now be quantitatively examined. As noted above, for Na^+ and K^+, it was found that Ser, Thr, Asp, Asn, Glu, Gln, and His all showed enhanced binding compared to values predicted from the polarizability correlation. Indeed, the bond energies of Na^+ and K^+ to Ser, Thr, Asp, Glu, and His form a series that parallels that for the aliphatic amino acids shown in Figure 4. For these amino acids, the average enhancement is about 28 and 24 kJ/mol for Na^+ and K^+, respectively.[11,12] Asn and Gln form a separate series in between the polar and aliphatic series, consistent with the lower dipole moment of the carboxamide side chain group compared to a carboxylic acid side chain group. As shown in Figure 5, comparable results are obtained for Rb^+ and Cs^+ for Ser, Thr, and His, where data are available.[12,16,17] Not surprisingly, the enhancements for these polar side chains relative to the aliphatic amino acids are smaller

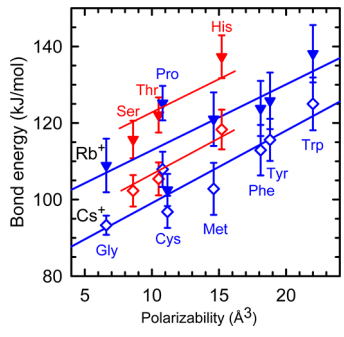

Figure 5. Experimental 0 K bond dissociation energies (in kJ/mol) for M^+(Gly), M^+(Pro), M^+(Cys), M^+(Met), M^+(Phe), M^+(Tyr), and M^+(Trp) (in blue) and M^+(Ser), M^+(Thr), and M^+(His) (in red) for $M^+ = Rb^+$ (solid triangles) and Cs^+ (open diamonds) are plotted versus the calculated polarizability volume of the amino acid (in Å^3). Lines (blue) through the aliphatic amino acids are linear regression fits to data for each metal cation. Lines (red) through the polar amino acids have the same slope but are displaced upward by 10 (Rb^+) and 7 (Cs^+) kJ/mol.

dx.doi.org/10.1021/jp401366g | J. Phys. Chem. B 2013, 117, 3771−3781

than those for the smaller more tightly binding alkali cations, specifically 10 and 7 kJ/mol for Rb^+ and Cs^+, respectively. The decrease is presumably a consequence of both the larger metal cation radius and the fact that the larger cations cannot take advantage of binding in a tridentate conformation as well as the smaller cations, as previously demonstrated elsewhere.[16,17]

CONCLUSION

The kinetic energy dependences of the collision-induced dissociation of Rb^+(AA) and Cs^+(AA), where AA = Met, Phe, Tyr, and Trp, are examined in a guided ion beam tandem mass spectrometer. The only dissociation pathway observed is loss of the intact amino acid from the complex. Rb^+−AA and Cs^+−AA BDEs at 0 and 298 K for these complexes are obtained by detailed modeling of the experimental cross sections. The thresholds for binding to the amino acids follow the order of M^+(Met) < M^+(Phe) < M^+(Tyr) < M^+(Trp), in agreement with quantum chemical calculations. When the def2-TZVPPD basis set is used, B3LYP, M06, and MP2(full) approaches including zero-point energy corrections and counterpoise corrections for basis set superposition errors generally agree well with our experimental values, Table 3, providing lower (B3LYP) and upper (M06 and MP2) limits, respectively, to the experimental values. MP2 results describe the relative binding energies of these four amino acids slightly better than the B3LYP approach, which tends to overestimate binding to Met.

The binding energies for these four amino acids to the alkali cations, Na^+, K^+, Rb^+, and Cs^+, exhibit the expected trend that they decrease as the metal cation increases in size. A good correlation between these BDEs and the polarizability of the amino acid is found. This correlation then allows the enhancement in binding afforded by more polar side chains to be quantatively assessed, with average enhancements of 10 and 7 kJ/mol for Rb^+ and Cs^+, respectively, to Ser, Thr, and His. These values are considerably lower than those to Na^+ and K^+ (28 and 24 kJ/mol, respectively, which is consistent with previous conclusions that the larger rubidium and cesium cations cannot take full advantage of binding in a tridentate conformation.[16,17]

ASSOCIATED CONTENT

Supporting Information

Text describing the general experimental procedures and thermochemical analysis procedures used. Tables of theoretical geometries and relative energies for rubidium and cesium-cation bound Met, Phe, Tyr, and Trp. Tables of bond energies calculated at alternative levels of theory and 298 K enthalpies and free energies of dissociation for various complex conformations. Figures of experimental results and data analysis for all eight metal cation-amino acid systems. This material is available free of charge via the Internet at http://pubs.acs.org.

AUTHOR INFORMATION

Notes

The authors declare no competing financial interest.

ACKNOWLEDGMENTS

This work is supported by the National Science Foundation, CHE-0911191 (MTR) and CHE-1049580 (PBA). A grant of computer time from the Center for High Performance Computing at the University of Utah is gratefully acknowledged.

REFERENCES

(1) Hood, S. L.; Comar, C. L. Metabolism of Cesium-137 in Rats and Farm Animals. *Arch. Biochem. Biophys.* **1953**, *45*, 423−433.
(2) Beauge, L. A.; Sjodin, R. A. Transport of Caesium in Frog Muscle. *J. Physiol.* **1968**, *194*, 105−123.
(3) Matsuda, H.; Matsuura, H.; Noma, A. Triple-barrel Structure of Inwardly Rectifying K^+ Channels Revealed by Cs^+ and Rb^+ Block in Guinea-pig Heart Cells. *J. Physiol.* **1989**, *413*, 139−157.
(4) Spruce, A. E.; Standen, N. B.; Stanfield, P. R. Rubidium Ions and the Gating of Delayed Rectifier Potassium Channels of Frog Skeletal Muscle. *J. Physiol.* **1989**, *411*, 597−610.
(5) Relman, S. R.; Lambie, A. T.; Burrows, B. A.; Roy, A. M. Cation Accumulation by Muscle Tissue: the Displacement of Potassium by Rubidium and Cesium in the Living Animal. *J. Clin. Invest.* **1957**, *36*, 1249−1256.
(6) Richmond, C. R. Retention and Excretion of Radionuclides of the Alkali Metals by Five Mammalian Species. *Health Phys.* **1980**, *38*, 1111−1153.
(7) Yen, C. K.; Budinger, T. F. Evaluation of Blood-brain Barrier Permeability Changes in Rhesus Monkeys and Man using ^{82}Rb and Positron Emission Tomography. *J. Comput. Assist. Tomogr.* **1981**, *5*, 792−799.
(8) Gal, J.-F.; Maria, P.-C.; Massi, L.; Mayeux, C.; Burk, P.; Tammiku-Taul, J. Cesium Cation Affinities and Basicities. *Int. J. Mass Spectrom.* **2007**, *267*, 7−23.
(9) Rodgers, M. T.; Armentrout, P. B. A Thermodynamic "Vocabulary" for Metal Ion Interactions in Biological Systems. *Acc. Chem. Res.* **2004**, *37*, 989−998.
(10) Ruan, C.; Rodgers, M. T. Cation-π Interactions: Structures and Energetics of Complexation of Na^+ and K^+ with the Aromatic Amino Acids, Phenylalanine, Tyrosine and Tryptophan. *J. Am. Chem. Soc.* **2004**, *126*, 14600−14610.
(11) Armentrout, P. B.; Gabriel, A.; Moision, R. M. An Experimental and Theoretical Study of Alkali Metal Cation/Methionine Interactions. *Int. J. Mass Spectrom.* **2009**, *283*, 56−68.
(12) Armentrout, P. B.; Citir, M.; Chen, Y.; Rodgers, M. T. Thermochemistry of Alkali Metal Cation Interactions with Histidine: Influence of the Side-Chain. *J. Phys. Chem. A* **2012**, *116*, 11823−11832.
(13) Moision, R. M.; Armentrout, P. B. An Experimental and Theoretical Dissection of Sodium Cation/Glycine Interactions. *J. Phys. Chem. A* **2002**, *106*, 10350−10362.
(14) Moision, R. M.; Armentrout, P. B. An Experimental and Theoretical Dissection of Potassium Cation/Glycine Interactions. *Phys. Chem. Chem. Phys.* **2004**, *6*, 2588−2599.
(15) Rodgers, M. T.; Armentrout, P. B. A Critical Evaluation of the Experimental and Theoretical Determination of Lithium Cation Affinities. *Int. J. Mass Spectrom.* **2007**, *267*, 167−182.
(16) Bowman, V. N.; Heaton, A. L.; Armentrout, P. B. Metal Cation Dependence of Interactions with Amino Acids: Bond Energies of Rb^+ to Gly, Ser, Thr, and Pro. *J. Phys. Chem. B* **2010**, *114*, 4107−4114.
(17) Armentrout, P. B.; Chen, Y.; Rodgers, M. T. Metal Cation Dependence of Interactions with Amino Acids: Bond Energies of Cs^+ to Gly, Pro, Ser, Thr, and Cys. *J. Phys. Chem. A* **2012**, *116*, 3989−3999.
(18) Moision, R. M.; Armentrout, P. B. The Special Five-membered Ring of Proline: An Experimental and Theoretical Investigation of Alkali Metal Cation Interactions with Proline and Its Four- and Six-membered Ring Analogues. *J. Phys. Chem. A* **2006**, *110*, 3933−3946.
(19) Ye, S. J.; Clark, A. A.; Armentrout, P. B. An Experimental and Theoretical Investigation of Alkali Metal Cation Interactions with Hydroxyl Side Chain Amino Acids. *J. Phys. Chem. B* **2008**, *112*, 10291−10302.
(20) Armentrout, P. B.; Armentrout, E. I.; Clark, A. A.; Cooper, T. E.; Stennett, E. M. S.; Carl, D. R. An Experimental and Theoretical Study of Alkali Metal Cation Interactions with Cysteine. *J. Phys. Chem. B* **2010**, *114*, 3927−3937.
(21) Kapota, C.; Lemaire, J.; Maitre, P.; Ohanessian, G. Vibrational Signature of Charge Solvation vs Salt Bridge Isomers of Sodiated

Amino Acids in the Gas Phase. *J. Am. Chem. Soc.* **2004**, *126*, 1836−1842.
(22) Armentrout, P. B.; Rodgers, M. T.; Oomens, J.; Steill, J. D. Infrared Multiphoton Dissociation Spectroscopy of Cationized Serine: Effects of Alkali-Metal Cation Size on Gas-Phase Conformation. *J. Phys. Chem. A* **2008**, *112*, 2248−2257.
(23) Rodgers, M. T.; Armentrout, P. B.; Oomens, J.; Steill, J. D. Infrared Multiphoton Dissociation Spectroscopy of Cationized Threonine: Effects of Alkali-Metal Cation Size on Gas-Phase Conformation. *J. Phys. Chem. A* **2008**, *112*, 2258−2267.
(24) Citir, M.; Stennett, E. M. S.; Oomens, J.; Steill, J. D.; Rodgers, M. T.; Armentrout, P. B. Infrared Multiple Photon Dissociation Spectroscopy of Cationized Cysteine: Effects of Metal Cation Size on Gas-Phase Conformation. *Int. J. Mass Spectrom.* **2010**, *297*, 9−17.
(25) Carl, D. R.; Cooper, T. E.; Oomens, J.; Steill, J. D.; Armentrout, P. B. Infrared Multiple Photon Dissociation Spectroscopy of Cationized Methionine: Effects of Alkali-Metal Cation Size on Gas-Phase Conformation. *Phys. Chem. Chem. Phys.* **2010**, *12*, 3384−3398.
(26) Heaton, A. L.; Bowman, V. N.; Oomens, J.; Steill, J. D.; Armentrout, P. B. Infrared Multiphoton Dissociation Spectroscopy of Cationized Asparagine: Effects of Alkali-Metal Cation Size on Gas-Phase Conformation. *J. Phys. Chem. A* **2009**, *113*, 5519−5530.
(27) Citir, M.; Hinton, C. S.; Oomens, J.; Steill, J. D.; Armentrout, P. B. Infrared Multiple Photon Dissociation Spectroscopy of Cationized Histidine: Effects of Metal Cation Size on Gas-Phase Conformation. *J. Phys. Chem. A* **2012**, *116*, 1532−1541.
(28) Forbes, M. W.; Bush, M. F.; Polfer, N. C.; Oomens, J.; Dunbar, R. C.; Williams, E. R.; Jockusch, R. A. Infrared Spectroscopy of Arginine Cation Complexes: Direct Observation of Gas-Phase Zwitterions. *J. Phys. Chem. A* **2007**, *111*, 11759−11770.
(29) Polfer, N. C.; Oomens, J.; Dunbar, R. C. IRMPD Spectroscopy of Metal-Ion/Tryptophan Complexes. *Phys. Chem. Chem. Phys.* **2006**, *8*, 2744−2751.
(30) Dunbar, R. C.; Steill, J. D.; Oomens, J. Cationized Phenylalanine Conformations Characterized by IRMPD and Computation for Singly and Doubly Charged Ions. *Phys. Chem. Chem. Phys.* **2010**, *12*, 13383−13393.
(31) Polfer, N. C.; Paizs, B.; Snoek, L. C.; Compagnon, I.; Suhai, S.; Meijer, G.; von Helden, G.; Oomens, J. Infrared Fingerprint Spectroscopy and Theoretical Studies of Potassium Ion Tagged Amino Acids and Peptides in the Gas Phase. *J. Am. Chem. Soc.* **2005**, *127*, 8571−8579.
(32) Rodgers, M. T. Substituent Effects in the Binding of Alkali Metal Ions to Pyridines Studied by Threshold Collision-Induced Dissociation and Ab Initio Theory: The Methylpyridines. *J. Phys. Chem. A* **2001**, *105*, 2374−2383.
(33) Moision, R. M.; Armentrout, P. B. An Electrospray Source for Thermochemical Investigation with the Guided Ion Beam Mass Spectrometer. *J. Am. Soc. Mass Spectrom.* **2007**, *18*, 1124−1134.
(34) Ye, S. J.; Armentrout, P. B. Absolute Thermodynamic Measurements of Alkali Metal Cation Interactions with a Simple Dipeptide and Tripeptide. *J. Phys. Chem. A* **2008**, *112*, 3587−3596.
(35) Heaton, A. L.; Moision, R. M.; Armentrout, P. B. Experimental and Theoretical Studies of Sodium Cation Interactions with the Acidic Amino Acids and Their Amide Derivatives. *J. Phys. Chem. A* **2008**, *112*, 3319−3327.
(36) Carl, D. R.; Moision, R. M.; Armentrout, P. B. Binding Energies for the Inner Hydration Shells of Ca^{2+}: An Experimental and Theoretical Investigation of $Ca^{2+}(H_2O)_x$ Complexes (x = 5 − 9). *Int. J. Mass Spectrom.* **2007**, *265*, 308−325.
(37) Chen, Y.; Rodgers, M. T. Structural and Energetic Effects in the Molecular Recognition of Protonated Peptidomimetic Bases by 18-Crown-6. *J. Am. Chem. Soc.* **2012**, *134*, 2313−2324.
(38) Chen, Y.; Rodgers, M. T. Structural and Energetic Effects in the Molecular Recognition of Amino Acids by 18-Crown-6. *J. Am. Chem. Soc.* **2012**, *134*, 5863−5875.
(39) Aristov, N.; Armentrout, P. B. Collision Induced Dissociation of Vanadium Monoxide Ion. *J. Phys. Chem.* **1986**, *90*, 5135−5140.
(40) Dalleska, N. F.; Honma, K.; Sunderlin, L. S.; Armentrout, P. B. Solvation of Transition Metal Ions by Water. Sequential Binding Energies of $M^+(H_2O)_x$ (x = 1−4) for M = Ti - Cu Determined by Collision-Induced Dissociation. *J. Am. Chem. Soc.* **1994**, *116*, 3519−3528.
(41) Daly, N. R. Scintillation Type Mass Spectrometer Ion Detector. *Rev. Sci. Instrum.* **1960**, *31*, 264−267.
(42) Ervin, K. M.; Armentrout, P. B. Translational Energy Dependence of $Ar^+ + XY \rightarrow ArX^+ + Y$ (XY = H_2, D_2, HD) from Thermal to 30 eV c.m. *J. Chem. Phys.* **1985**, *83*, 166−189.
(43) Loh, S. K.; Hales, D. A.; Lian, L.; Armentrout, P. B. Collision-Induced Dissociation of Fe_n^+ (n = 2 - 10) with Xe: Ionic and Neutral Iron Cluster Binding Energies. *J. Chem. Phys.* **1989**, *90*, 5466−5485.
(44) Khan, F. A.; Clemmer, D. E.; Schultz, R. H.; Armentrout, P. B. Sequential Bond Energies of $Cr(CO)_x^+$, x = 1−6. *J. Phys. Chem.* **1993**, *97*, 7978−7987.
(45) Rodgers, M. T.; Ervin, K. M.; Armentrout, P. B. Statistical Modeling of Collision-induced Dissociation Thresholds. *J. Chem. Phys.* **1997**, *106*, 4499−4508.
(46) Armentrout, P. B.; Ervin, K. M.; Rodgers, M. T. Statistical Rate Theory and Kinetic Energy-Resolved Ion Chemistry − Theory and Applications. *J. Phys. Chem. A* **2008**, *112*, 10071−10085.
(47) Frisch, M. J.; Trucks, G. W.; Schlegel, H. B.; Scuseria, G. E.; Robb, M. A.; Cheeseman, J. R.; Scalmani, G.; Barone, V.; Mennucci, B.; Petersson, G. A. et al. *Gaussian 09*, Revision A.02; Gaussian Inc.; Pittsburgh, PA, 2009.
(48) Gapeev, A.; Dunbar, R. C. Cation-π Interactions and the Gas-Phase Thermochemistry of the Na^+/Phenylalanine Complex. *J. Am. Chem. Soc.* **2001**, *123*, 8360−8365.
(49) Dunbar, R. C. Complexation of Na^+ and K^+ to Aromatic Amino Acids: A Density Functional Computational Study of Cation-π Interactions. *J. Phys. Chem. A* **2000**, *104*, 8067−8074.
(50) Becke, A. D. Density-functional Thermochemistry. III. The Role of Exact Exchange. *J. Chem. Phys.* **1993**, *98*, 5648−5652.
(51) Lee, C.; Yang, W.; Parr, R. G. Development of the Colle-Salvetti Correlation-energy Formula into a Functional of the Electron Density. *Phys. Rev. B* **1988**, *37*, 785−789.
(52) Armentrout, P. B.; Austin, C. A.; Rodgers, M. T. Alkali Metal Cation Interactions with 12-Crown-4 in the Gas Phase: Revisited. *Int. J. Mass Spectrom.* **2013**, *330*−*332*, 16−26.
(53) Weigend, F.; Ahlrichs, R. Def2-SVP basis sets. *Phys. Chem. Chem. Phys.* **2005**, *7*, 3297−3305.
(54) Rappoport, D.; Furche, F. Property-optimized Gaussian Basis Sets for Molecular Response Calculations. *J. Chem. Phys.* **2010**, *133*, 134105.
(55) Leininger, T.; Nicklass, A.; Kuechle, W.; Stoll, H.; Dolg, M.; Bergner, A. The Accuracy of the Pseudopotential Approximation: Non-frozen-core Effects for Spectroscopic Constants of Alkali Fluorides XF (X = K, Rb, Cs). *Chem. Phys. Lett.* **1996**, *255*, 274−280.
(56) Feller, D. The Role of Databases in Support of Computational Chemistry Calculations. *J. Comput. Chem.* **1996**, *17*, 1571−1586.
(57) Schuchardt, K. L.; Didier, B. T.; Elsethagen, T.; Sun, L.; Gurumoorthi, V.; Chase, J.; Li, J.; Windus, T. L. Basis Set Exchange: A Community Database for Computational Sciences. *J. Chem. Inf. Model.* **2007**, *47*, 1045−1052.
(58) Foresman, J. B.; Frisch, A. E. *Exploring Chemistry with Electronic Structure Methods*, 2nd ed.; Gaussian, Inc.: Pittsburgh, PA, 1996.
(59) Zhao, Y.; Truhlar, D. G. The M06 Suite of Density Functionals for Main Group Thermochemistry, Thermochemical Kinetics, Noncovalent Interactions, Excited States, and Transition Elements: Two New Functionals and Systematic Testing of Four M06-class Functionals and 12 Other Functionals. *Theor. Chem. Acc.* **2008**, *120*, 215−241.
(60) Möller, C.; Plesset, M. S. Note on an Approximation Treatment for Many-electron Systems. *Phys. Rev.* **1934**, *46*, 618−622.
(61) Boys, S. F.; Bernardi, R. The Calculation of Small Molecular Interactions by the Differences of Separate Total Energies. Some Procedures with Reduced Errors. *Mol. Phys.* **1970**, *19*, 553−566.

(62) van Duijneveldt, F. B.; van Duijneveldt-van de Rijdt, J. G. C. M.; van Lenthe, J. H. State of the Art in Counterpoise Theory. *Chem. Rev.* **1994**, *94*, 1873−1885.
(63) Hoyau, S.; Norrman, K.; McMahon, T. B.; Ohanessian, G. A Quantitative Basis for a Scale of Na^+ Affinities of Organic and Small Biological Molecules in the Gas Phase. *J. Am. Chem. Soc.* **1999**, *121*, 8864−8875.
(64) Feller, D.; Glendening, E. D.; Woon, D. E.; Feyereisen, M. W. An Extended Basis Set Ab Initio Study of Alkali Metal Cation−water Clusters. *J. Chem. Phys.* **1995**, *103*, 3526−3542.
(65) Feller, D. A Complete Basis Set Estimate of Cation-bond Strengths: Na^+(ethylene) and Na^+(benzene). *Chem. Phys. Lett.* **2000**, *322*, 543−548.
(66) McMahon, T. B.; Ohanessian, G. An Experimental and Ab Initio Study of the Nature of the Binding in Gas-Phase Complexes of Sodium Ions. *Chem.—Eur. J.* **2000**, *6*, 2931−2941.
(67) Hay, P. J.; Wadt, W. R. Ab Initio Effective Core Potentials for Molecular Calculations. Potentials for K to Au Including the Outermost Core Orbitals. *J. Chem. Phys.* **1985**, *82*, 299−310.
(68) Glendening, E. D.; Feller, D.; Thompson, M. A. An Ab Initio Investigation of the Structure and Alkali Metal Cation Selectivity of 18-Crown-6. *J. Am. Chem. Soc.* **1994**, *116*, 10657−10669.
(69) Lifshitz, C. Recent Developments in Applications of RRKM-QET. *Adv. Mass Spectrom.* **1989**, *11*, 713−729.
(70) Wilson, R. G.; Brewer, G. R. *Ion Beams with Applications to Ion Implantation*; Wiley: New York, 1973.
(71) Heaton, A. L.; Armentrout, P. B. Experimental and Theoretical Studies of Potassium Cation Interactions with the Acidic Amino Acids and Their Amide Derivatives. *J. Phys. Chem. B* **2008**, *112*, 12056−12065.